Novel biomaterials: plasma-enabled nanostructures and functions

2016 J. Phys. D: Appl. Phys. 49 273001

(http://iopscience.iop.org/0022-3727/49/27/273001)

IOP Publishing Journal of Physics D: Applied Physics
J. Phys. D: Appl. Phys. **49** (2016) 273001 (16pp) doi:10.1088/0022-3727/49/27/273001

Topical Review

Novel biomaterials: plasma-enabled nanostructures and functions

Igor Levchenko[1], Michael Keidar[2], Uroš Cvelbar[3], Davide Mariotti[4], Anne Mai-Prochnow[5], Jinghua Fang[6] and Kostya (Ken) Ostrikov[1,7,8]

[1] School of Chemistry, Physics, and Mechanical Engineering Queensland University of Technology, Brisbane, Queensland 4000, Australia
[2] George Washington University, 20052, Washington, DC, USA
[3] Jozef Stefan Institute, Jamova cesta 39, SI-1000 Ljubljana, Slovenia
[4] Nanotech. & Integrated Bio-Eng. Centre (NIBEC), University of Ulster, Shore Road, Newtownabbey, UK
[5] CSIRO Manufacturing Flagship, PO Box 218, Lindfield, NSW 2070, Australia
[6] School of Mathematical and Physical Sciences, Faculty of Science, University of Technology Sydney, Ultimo, NSW 2007, Australia
[7] Joint CSIRO – QUT Sustainable Materials and Devices Laboratory, Commonwealth Scientific and Industrial Research Organisation, PO Box 218, Lindfield, New South Wales 2070, Australia
[8] Beijing National Laboratory for Molecular Sciences (BNLMS), College of Chemistry and Molecular Engineering, Peking University, Beijing 100871, People's Republic of China

E-mail: Igor.Levchenko@qut.edu.au

Received 11 February 2016, revised 24 April 2016
Accepted for publication 27 April 2016
Published 7 June 2016

Abstract

Material processing techniques utilizing low-temperature plasmas as the main process tool feature many unique capabilities for the fabrication of various nanostructured materials. As compared with the neutral-gas based techniques and methods, the plasma-based approaches offer higher levels of energy and flux controllability, often leading to higher quality of the fabricated nanomaterials and sometimes to the synthesis of the hierarchical materials with interesting properties. Among others, nanoscale biomaterials attract significant attention due to their special properties towards the biological materials (proteins, enzymes), living cells and tissues. This review briefly examines various approaches based on the use of low-temperature plasma environments to fabricate nanoscale biomaterials exhibiting high biological activity, biological inertness for drug delivery system, and other features of the biomaterials make them highly attractive. In particular, we briefly discuss the plasma-assisted fabrication of gold and silicon nanoparticles for bio-applications; carbon nanoparticles for bioimaging and cancer therapy; carbon nanotube-based platforms for enzyme production and bacteria growth control, and other applications of low-temperature plasmas in the production of biologically-active materials.

Keywords: nanoscale biomaterials, low-temperature plasma, nanoparticles, carbon nanotubes, proteins

(Some figures may appear in colour only in the online journal)

1. Introduction

Biomaterials are novel materials featuring high biological activity, high biocompatibility, inertness or other properties that make them attractive for various biology, biotechnology and medicine-related applications, such as drug delivery devices [1, 2], production of enzymatic biocatalysts [3, 4], designing bioreactors [5, 6], biosensors [7, 8], biofilms [9, 10], nanostructured platforms for the advanced bioreactors [11], next-generation nanobiointerfaces [12, 13], biocompatible materials and systems [14, 15], antibacterial materials [16, 17] and many others. Plasma-based techniques are promising for biomaterial production due to higher levels of particle energy and material controllability, as compared with the traditional neutral-gas based production methods [18, 19]. Unique properties of the low-temperature plasma environment ensure synthesis of the biomaterials with interesting properties [20, 21].

Here we briefly review the methods and biomaterials which can be fabricated using low-temperature plasmas, making the main stress to the unique capabilities of plasma-based tools and processes resulting in the synthesis of biomaterials and bioplatforms. Metal and carbon nanoparticles, complex carbon nanotube-based platforms, surface-engineered silicon nanocrystals, hierarchical plasma-treated gold-silver structures for protein retention will be among others considered. Besides, plasma functionalization and direct influence of the plasma fluxes onto living cells and biofilms will be discussed, in view to better understand the unique capabilities of the plasma-based techniques for biomaterial fabrication.

2. Plasma—a tool for building and control

In this section we will examine several kinds of nanostructures and nanostructured materials created with the use of methods and techniques based on low-temperature plasmas. Both technological aspects and material properties are considered.

2.1. Surface-grown arrays of gold and silicon nanoparticles for bio-applications: plasma drives self-organization

Gold nanoparticles are the recently synthesized nanomaterials demonstrating significant potential for cancer therapy [22, 23], biosensing [24], biocatalysis [25]. The arrays of gold nanoparticles grown on surfaces may be used for bio-detection [26], biosensing [27], bioelectronics [28] and many others applications, including catalytic systems for the nucleation and growth of carbon nanotubes [29]. Gold nanorods are also of interest which could be used, e.g. as contrast agents for multimodal imaging [30]. Structural and morphological properties of such arrays, including ordering are of particular importance [31, 32]. Several dedicated experiments have proven that the plasma-based techniques lead to results superior to those obtained by traditional chemical vapour deposition (CVD) methods.

How can low-temperature plasma help to produce high-quality nanoparticles? The inductively-coupled plasma (ICP) technique was successfully used to produce high-quality

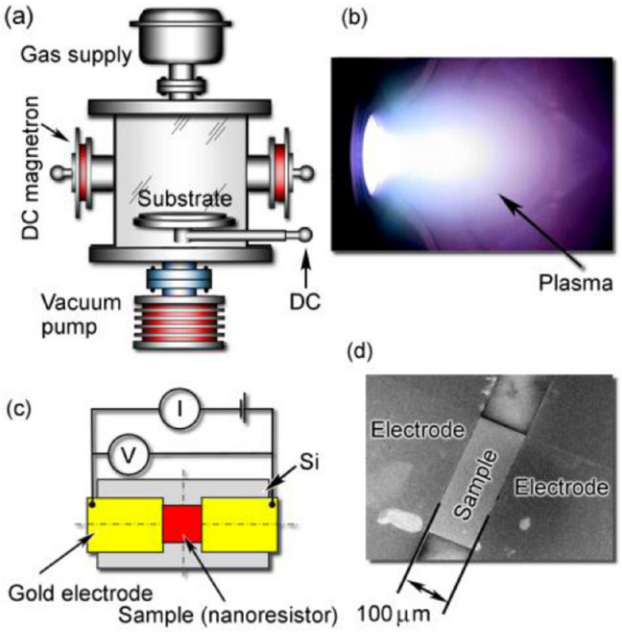

Figure 1. (a) Schematic of the experimental setup for depositing nanoparticle gold films suitable for the use as e.g. biosensors. (b) Photo of the magnetron discharge. (c) Scheme of the sample design and electrical measurements. (d) Optical microscopy image of the sample fabricated by the multiple deposition-annealing process. Reprinted with permission from [33]. Copyright 2011 AIP Publishing.

arrays of gold nanoparticles on silicon surfaces, and to enhance the array ordering. Multiple deposition-annealing process was used to form patterns of gold nanoparticles with different morphology and density. The process was controlled by varying the deposition time and the post-processing temperature. The morphology of the deposit was controlled by initiating nanoparticle nucleation and growth between the already existing nanostructures. Hence, control over the pattern structure was ensured due to plasma-specific effects.

The pattern of gold nanoparticles was formed on silica (silicon oxide) surface in a direct current magnetron discharge. Argon was used as a process gas at a pressure of 1 Pa. The processed surface was biased with direct current potential of −50 V. The experimental setup is illustrated in figure 1(a). Vacuum pump and gas supply system were used to maintain the pressure during the deposition and treatment. A photo of the DC magnetron discharge is presented in figure 1(b). The nanoparticle patterns were formed on a narrow specimen of about 1 mm long and 0.2 mm wide, made of a silicon substrate covered with a silica layer. Firstly, the samples were cleaned in acetone solution using ultrasonication, then the cleaning was repeated in ethanol and wafers were dried by nitrogen. After that, the samples were processed by the plasma in a chamber as described above. Four different samples were fabricated to study the effect of the plasma parameters onto the structure and morphology of the nanoparticle pattern.

The samples were fabricated using a different number of deposition/annealing cycles. Specifically, 12 nm gold layer was formed on the first sample by a single deposition/annealing repetition at 70 °C for 5 min. The next sample was fabricated by the doubled cycle resulted in 18 nm layer, and the rest samples had 21 and 22 nm, respectively. This method resulted in different

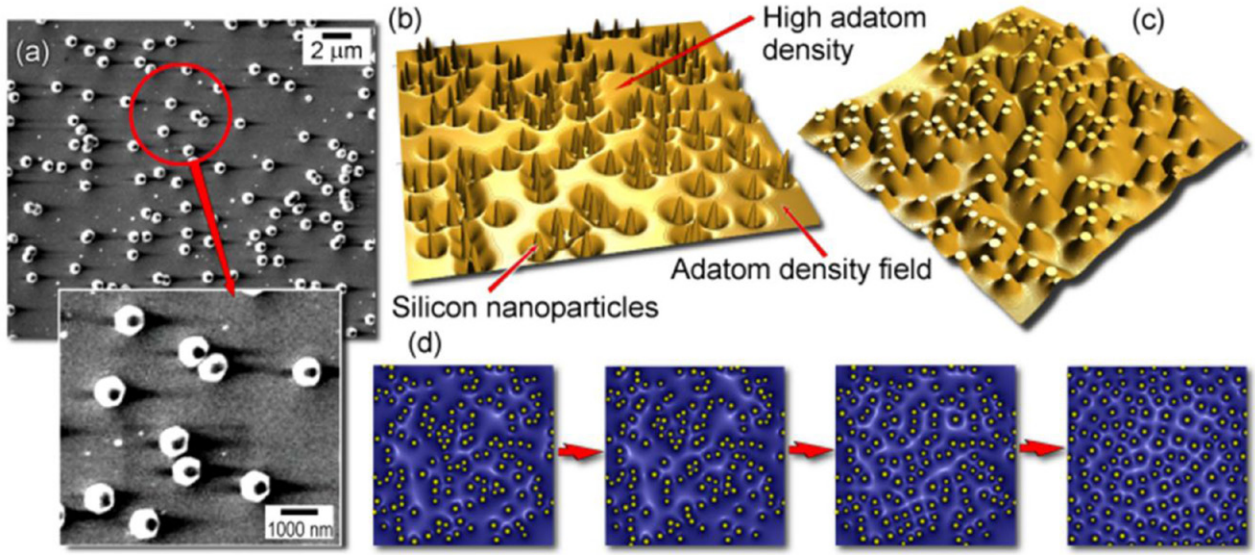

Figure 2. Scanning electron microscopy characterization and calculated 3D patterns of electric field and adatom density of silicon nanoparticles on a silica surface during the treatment in nitrogen + argon plasma. SEM images, low and high resolution (a). Calculated patterns of the adatom density field (b) and electric field (c); and four screenshots illustrating transformation of the electric field pattern during self-organizational ordering. The spatial ordering increases from left to right (d). Reprinted with permission from Levchenko *et al* [34]. Copyright 2011 IOP Publishing.

nanoparticle morphologies for different samples, thus *revealing the potential of plasma for the structure control*. Electrical characteristics of the sample were measured to check the possibility of fabricating sensor. The details of the design and electrical measurements are shown in figure 1(c). The optical photo of the fabricated sensor is shown in figure 1(d). More details on the process and results can be found elsewhere [33].

Plasmas ignited in the N_2+Ar gas mixture were used to produce patterns of silicon nanoparticles on silicon wafer [34, 35]. The scanning electron microscopy image of a typical silicon nanoparticle pattern formed by processing of a silicon surface in plasma at a surface temperature of 700 °C is shown in figure 2(a). The nanoparticles are distributed uniformly about the surface, and the surface density of the nanoparticles is low.

One specific feature of the plasma is a large amount of control parameters influencing the deposition process, and this makes the experiments time-consuming. To study in detail the potential of plasma-based methods for the formation of uniform nanoparticle patterns, simulations were used. Figures 2(b) and (c) present the 3D visualizations of the adsorbed atom (adatom) density field and the structure of the electric field, calculated using the diffusion-based model [36]. The image presents that the pattern of adatom density is quite irregular, and there are areas with a relatively high density of adatoms where new nanostructures may nucleate. The structure of the calculated electric field is illustrated in figure 2(c). The nucleation of new nanoparticles is highly probable in such non-uniform patterns, and specifically where the adatom density is high enough to ensure high collision density on the surface. Further treatment elevates the level of uniformity of nanoparticle patterns in such systems. Figure 2(d) presents several screenshots illustrating the change in the structure of electric field during the plasma treatment. Direct experiments on deposition of the patterns of gold nanoparticles on silica surface by magnetron sputtering also supported these results [34].

Are the plasma-related effects important in these processes? The detailed analysis have shown that just the plasma plays a major role in the formation of uniform nanoparticle patterns by ensuring the proper structure of ion fluxes to the substrate, and thus driving the self-organization [37, 38] on the surface by governing the electric field and diffusion which are the main drivers of self-organization [39]. Some more details on analysing self-organization are published in other articles [40, 41]. It could be stressed that the electric field can be varied by surface bias [42, 43], and thus the self-organization in the pattern of nanoparticles can be controlled by a proper selection of the *surface temperature and plasma parameters*, such as electron temperature and density.

2.2. Growth of carbon nanoparticles in plasma: levitation and tuned precipitation

Carbon nanoparticles are another example of the plasma-based fabrication of biologically relevant materials. In particular, carbon nanoparticles can be used in bioimaging applications [44], they can serve as fluorescent labels for applications in theranostics (integrated diagnosis and therapy) [45, 46] and cancer therapy [47]. They demonstrate excellent biocompatibility and can be used as active bioimaging agents [48] and means for nanomedicinal therapy [49, 50].

Is the plasma useful for the production of carbon nanoparticles? One of the typical processes resulting in the fabrication of carbon nanoparticles in low-temperature environment was implemented using asymmetric radio-frequency (RF) discharge at 13.56 MHz (4–20 W) [51]. An experimental setup comprised the vacuum and gas equipment, and the characterization system including laser diode-detector system capable of detecting nucleation and growth of nanoparticles in a plasma, and a Quantum cascade laser measurement and control system capable of measuring the plasma parameters directly during

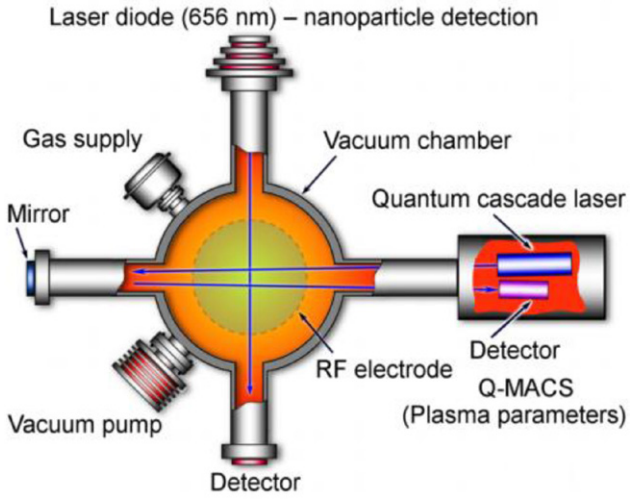

Figure 3. Experimental setup for nanoparticle nucleation and growth in acetylene plasma. The laser diode-based system was used to pass light through the dust and measure the density of nanoparticles in the plasma. The Quantum cascade laser measurement and control system provided information about time-dependent concentration of acetylene in the plasma. Reprinted with permission from Hundt *et al* [51]. Copyright 2011 AIP Publishing.

the process. This system is sketched in figure 3. In the process, argon and acetylene were used as a plasma-sustaining gas and reactive precursors. In this case the ion and neutral particle densities in plasma were 10^9 cm^{-3} and 10^7 cm^{-3}, respectively. The direct measurements in the similar setup and discharge have demonstrated a quite good agreement with the above mentioned density numbers [52].

Concentration of acetylene in the chamber was varied using the Quantum cascade laser measurement and gas control system. The quantum cascade laser was operated at the rate of 0.25 cm^{-1} within a spectral range around 1342 cm^{-1} where the spectral lines of the infrared active molecules are present. Specifically, the density of acetylene molecules was measured by the spectral line 1342.35 cm^{-1} [53]. The absolute density of acetylene molecules in the setup was achieved by fitting the absorption signal and comparing with the data stored in the database [54]. The sizes and distribution of nanoparticles nucleated and grown in the plasma were measured by transmitted light from laser beam detected by a photodiode in the integrated amplifier circuit. The intensity of light transmitted through the plasma decreases if the plasma region contains any nanoparticles. Scattering the light on nanoparticles reveals the presence of nanoparticles nucleated in the plasma.

Figure 4(a) is an optical photograph of the plasma region with the clouds of nucleated carbon nanoparticles. Laser beam illuminates the clouds and they are visible as two grey spots. It was found that the volume of the nanoparticle-containing areas changed during the process. The carbon nanoparticles then deposit onto the electrode when the plasma cannot ensure levitation, and can be collected from the surface for the further use. In figure 4(b) one can see the scanning electron microscopy image of the carbon nanoparticles collected from the surface in the chamber. Note very regular, near-spherical

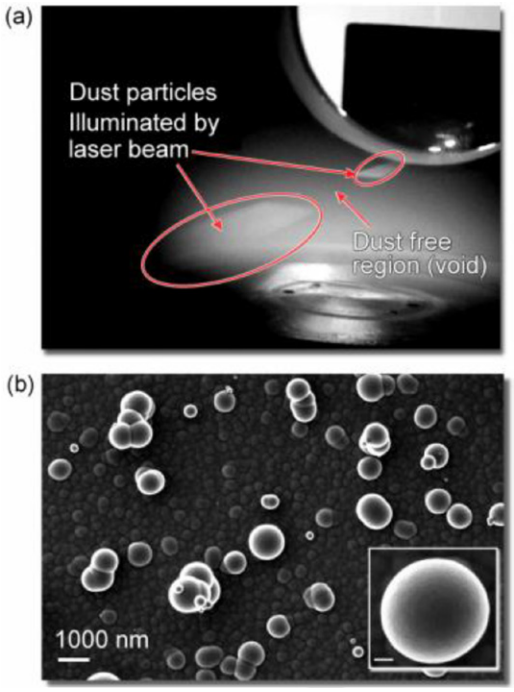

Figure 4. Optical and scanning electron microscopy images of dust growing in the plasma. (a) Optical photograph of a dust nucleated in the plasma, illuminated by laser. The nanoparticle free region is visible between the two dust clouds. (b) SEM image of typical carbon nanoparticles collected on a particle collector. The scale bar in the inset at the right lower corner is 200 nm. Reprinted with permission from Hundt *et al* [51]. Copyright 2011 AIP Publishing.

shape of the collected nanoparticles, typical for the structures nucleated without any contact with the solid surfaces (i.e. directly in the plasma).

How plasma-specific effects work in this technique? Plasma-related effects indeed play a key role in the main processes involved in this technique. It is believed that nanoparticles nucleate and grow in plasmas by the following scenario [55]. During the initial nucleation stage, the seed particles having several nm in diameter coalesce owing to the electric charge fluctuations in a plasma [56], and finally form larger particles of several tens of nanometers like it occurs in neutral aerosols. The driving force of the coagulation is plasma-induced electric charges which lead to the attraction between negatively charged nanoparticles and strong irregular ion fluxes [57, 58]. As a result, the nanoparticles reaching 1 μm may be nucleated and grown directly in plasmas, without contact with any surfaces or catalysts. It should be stressed that the volumetric concentration of such dust clouds is rather low and reaches (2–5) $\times$ 10^3 cm^{-3}. Moreover, larger nanoparticles have larger collision cross-sections, and hence they act as collectors of neutral and ionized particles from the plasma, thus growing to up to micrometre size [59]. Importantly, the size and mass distributions of the plasma-grown nanoparticles are typically quite uniform, as it can be observed in figure 4. The reason for this is the re-distribution of material fluxes between larger and smaller charged particles in the plasma. Thus, just the *plasma effect ensures nucleation and growth of size- and shape-uniform nanoparticles* [51].

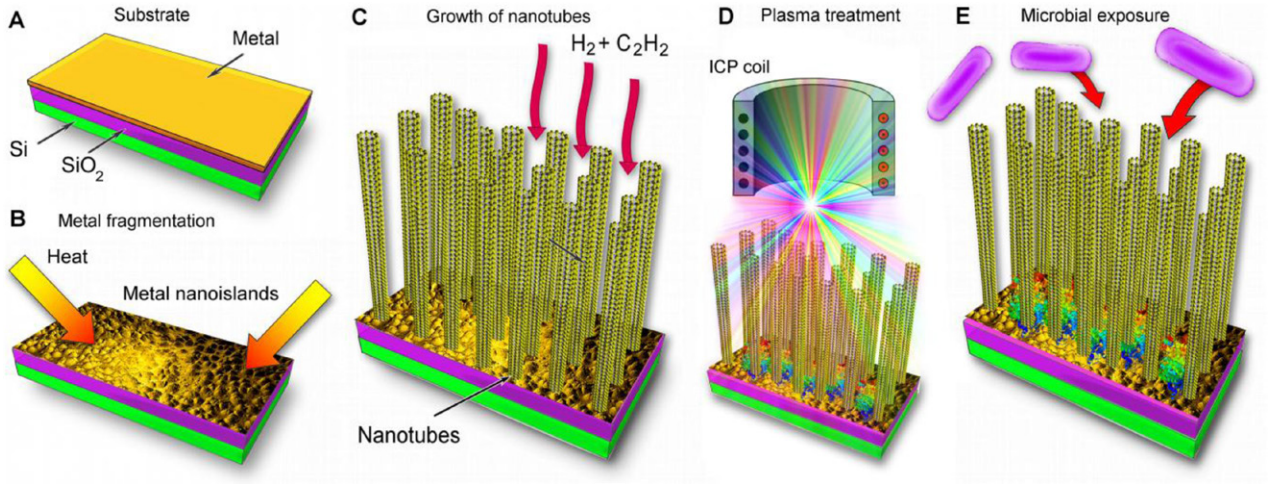

Figure 5. Schematic of the fabrication and plasma activation of carbon nanotube—metal platform. (a) Design of the layered substrate used for the growth of carbon nanotubes. (b) Continuous metal layer was heated to form array of metal particles to catalyze the nucleation of nanotubes. (c) Growth of carbon nanotubes on the fragmented metal catalyst in thermal furnace. (d) The ready array of carbon nanotubes is treated with inductively coupled plasma. (e) Microbial exposure of the platform. Reprinted with permission from Yick *et al* [68]. Copyright 2015 RSC.

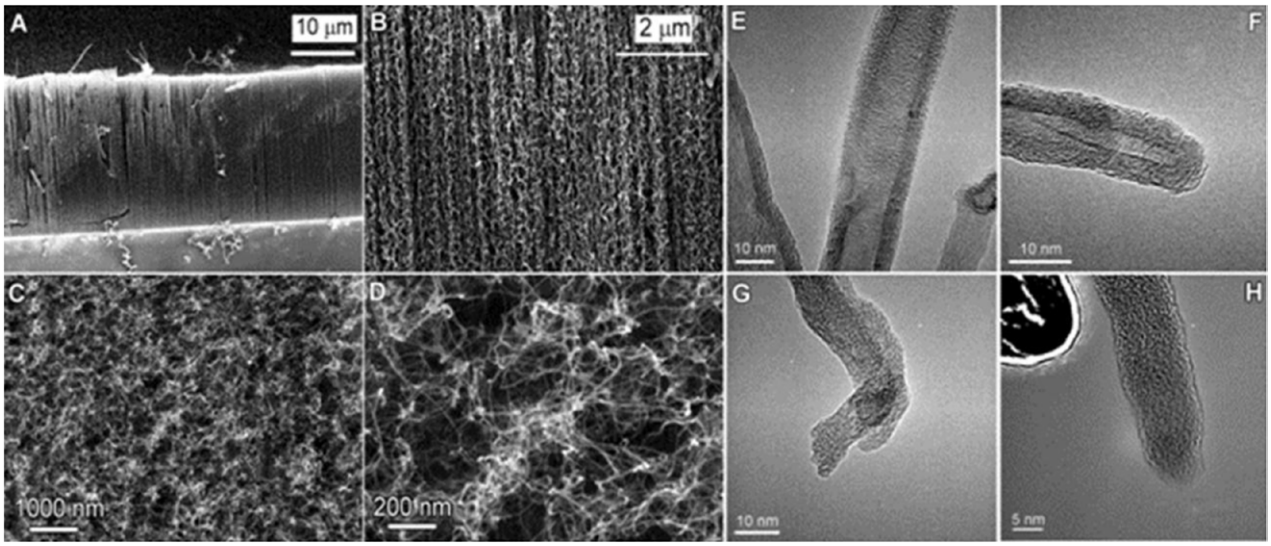

Figure 6. Electron microscopy characterization of the carbon nanotubes which form a part of the hybrid nanotube-metal platform. (a) and (b) Low- and high-resolution scanning electron microscopy images of as-prepared nanotube array (side views). (c) and (d) Top views of the as-prepared nanotube array. (e) and (f) High-resolution transmission electron microscopy images depicting pristine nanotubes, and (g) and (h) nanotubes after the plasma processing. Reprinted with permission from Yick *et al* [68]. Copyright 2015 RSC.

2.3. Carbon nanotube-based platforms for enzyme production and bacteria growth control

Let us examine how the *plasma-related effects work in building the nanostructured biotechnological platforms*. The platforms and materials based on carbon nanostructures such as patterns of vertically-aligned graphene flakes [60], single- and multi-wall carbon nanotubes [61], vertically-aligned carbon nanocones and other nanostructures comprising carbon honeycomb lattices have interesting characteristics [62–64] relevant to the advanced biotechnological platforms [65–67]. Described here is the hybrid metal-carbon nanotube plasma-activated system which could be a base for the biotechnological and biomedical platform. The vertically-aligned multiwall nanotubes determine the most important properties of this platform.

To build the carbon nanotube—metal platform, a conventional CVD technique was firstly used to prepare the base [68]. The thermally oxidized silicon wafer was firstly covered with a 10 nm layer of alumina. Then, a very thin (about 2 nm) layer of pure iron was sputtered onto the alumina [69]. The samples were then installed in the thermal furnace, and a forest of vertically-aligned carbon nanotubes was grown at a constant flow of hydrogen and acetylene mixture, under atmospheric-pressure conditions (see figure 5). More details on the platform fabrication can be found elsewhere [68]. The as-grown nanotube arrays were then treated with argon inductively coupled plasmas, as shown in figure 5(d). The ready sample was loaded into a process chamber where a constant argon flow was maintained at a pressure of 5 Pa. The low-temperature plasma was then ignited in argon gas, and the samples were processed for several minutes.

In figure 6 one can see the scanning and transmission electron microscopy images taken from the ready platform. The carbon nanotube pattern (forest) consists of multiwall nanotubes

which are in general vertically-aligned but somewhat entangled. The gaps between the nanotubes reach hundreds of nanometres. Apparently, the whole array is completely impenetrable for bacteria whose sizes are in the micrometre range. The side views of the nanotubes in figure 6(a) show that the whole forest is 20–25 μm in height, and the surface density reaches 5×10^{10} tubes $\times$ cm^{-2}. Importantly, the nanotubes are not absolutely straight but curved and entangled; this in turn makes the whole array even more impenetrable. The transmission electron microscopy has confirmed that the pristine nanotubes reach 10 nm in diameter and consist of up to 10 walls. Figures 6(e) and (f) which are also the TEM images confirm the presence of lattice fringes, thus proving highly ordered structure of the nanotubes. The plasma treatment did not change the diameter of carbon nanotubes, but significantly changed the internal structure, as it is seen in figures 6(g) and (h). Besides, the well-rounded tips of pristine nanotubes are opened after the plasma treatment.

The bacterial culture experiments were then performed using the above described platform after the plasma treatment. The four kinds of bacteria commonly used in similar experiments, namely *Bacillus subtilis*, *Escherichia coli*, *Staphylococcus epidermidis* and *Pseudomonas aeruginosa* were cultivated and tested. The detailed description of the bacterial cultures, as well as characterization procedures and techniques can be found in the relevant publication [68].

An open source software ImageJ was then used to calculate the area coverage of the grown bacterial colonies. The viability of the cultivated bacteria was then assessed by colony forming units [68]. The biofilms consisting of *E. coli* and *B. subtilis* bacteria on carbon nanotubes were then characterized by the flow cytometry technique. The biofilms were collected from the carbon nanotubes using sterile tools, and then sonicated in phosphate buffered saline. After breaking the clumps by sonication, they were analysed using LIVE/DEAD® BacLight™ staining according to the manufacturer's instructions. The percentage of viable cells was calculated.

The obtained results have demonstrated that the nanotube forests grown on silica and metal bases can form quite useful biotechnological platforms. Importantly, the behaviour of the vertically-aligned arrays of carbon nanotubes in the presence of a bacterial attack differs quite significantly from that of entangled, dispersed nanotubes. Indeed, the vertically-aligned nanotube forests did not demonstrate strong antibacterial activity. More importantly, they show selectivity towards the different bacteria forming the biofilms on top of the nanotube arrays. The above described experiments have demonstrated that the plasma treatment makes the vertically-aligned nanotubes discriminative toward the Gram-negative and Gram-positive bacteria. The Gram-positive bacteria (*B. subtilis* and *S. epidermidis* in the above discussed experiments) exhibited good biofilm formation ability and high numbers of viable bacteria on the platform after the plasma treatments, as seen in figure 7. On the other hand, the *E. coli* and *P. aeruginosa* bacteria (Gram-negative) have demonstrated no significant changes regardless of the presence of vertically-aligned carbon nanotubes and plasma processing.

This effect was explained by the structural differences in cell walls and membranes of these two kinds of bacteria. As a result of this difference (specifically, different thickness of the cell wall), the bacteria have demonstrated different responses to the treated and untreated carbon nanotubes. These experiments validated the ideas to use the dense, ordered nanotube arrays in the capacity of biotechnological platform capable to selectively control the growth of various biofilms and biocatalyst-producing bacterial cultures for biotechnological applications.

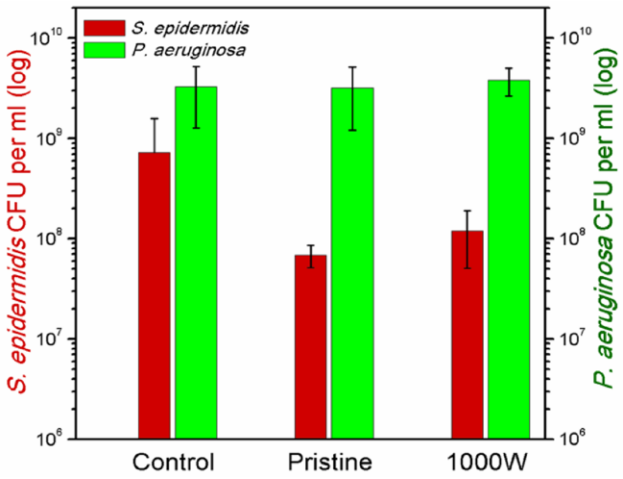

Figure 7. Number of colony forming units of *S. epidermidis* and *P. aeruginosa* bacteria sampled from the control, pristine, and plasma-treated carbon nanotube arrays. Reprinted with permission from Yick *et al* [68]. Copyright 2015 RSC.

To directly assess the protective effects of this platform against microbiological attacks, (this feature is of special importance when the platform is used for immobilization of enzymatic proteins), a dedicated experiment was conducted on the penetration of live bacteria (*B. subtilis*) into the nanotube pattern. The prepared and plasma-treated platforms were incubated in the solution with the live culture of *B. subtilis*, and the SEM images were made. Figure 8 shows the upper surface of the sample after 12 h in the shaker and critical point drying (a) and after drying in open air (b). Live bacteria cannot penetrate to the bottom where the enzymes are immobilized, and thus the bacterial protection is ensured by a simple mechanical method, as shown in figure 8(c). Figures 8(d) and (e) demonstrate that the bacteria indeed remain on the nanotube array surface. More information on the experiments on *B. subtilis* penetration in the nanotube pattern can be found elsewhere [70].

2.4. Plasma-engineered Si nanocrystals and Si nanocrystals—carbon nanotube compositions

Silicon nanocrystals are highly promising nano-objects which demonstrate many bio-related properties not achievable for other materials and systems. In particular, the silicon nanocrystals and nanoparticles can be useful for imaging of cancer cells [71], for controlling active oxygen in the biomedical applications [72, 73], for biosensing [74], single-molecule tracking [75], as biocompatible fluorescent nanolabels [76], delivery systems [77], and nutritional food additive [78]. Various aspects of the silicon nanoparticle interaction with

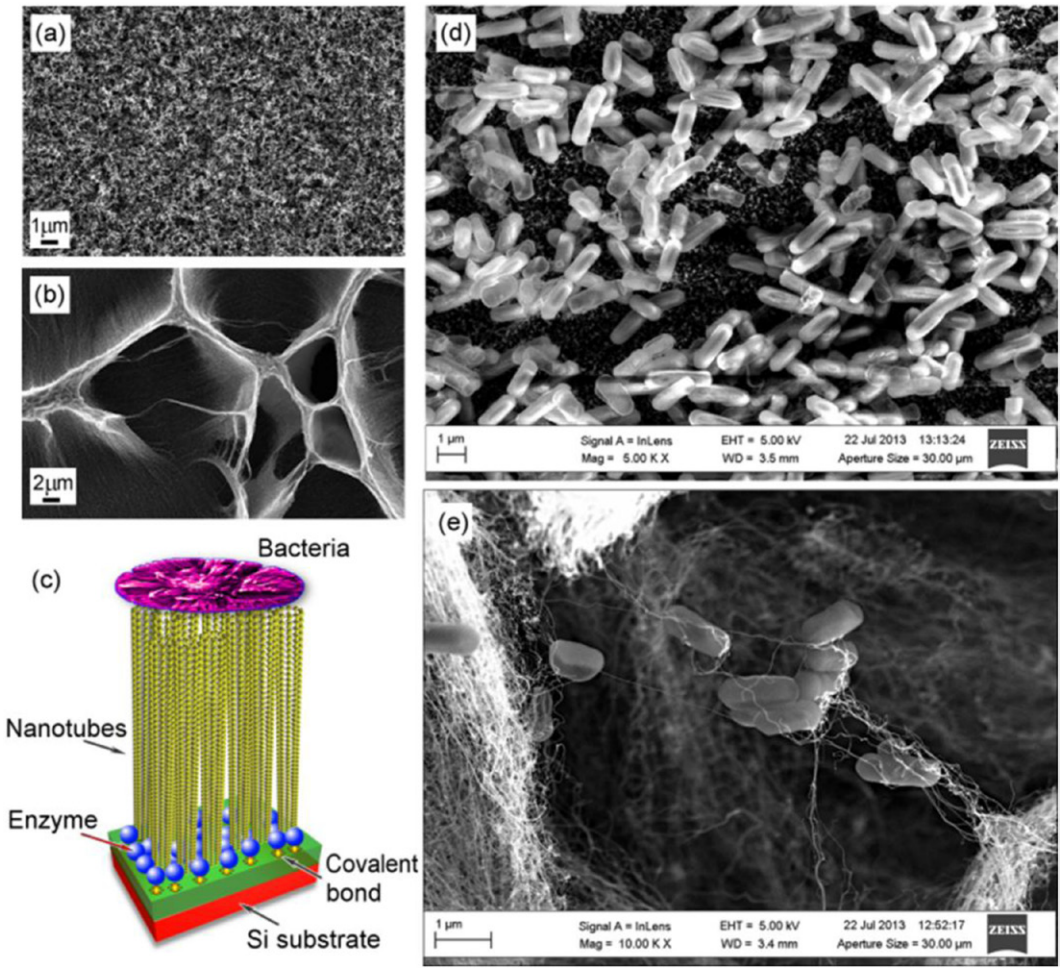

Figure 8. Experiments on bacterial attacks on the carbon nanotube-based platform. (a) SEM images of the upper surface of carbon nanotubes after holding in shaker and critical point drying and (b) after drying in open air. No changes in the structure of surface after critical point drying were found as compared with the as-prepared sample. (c) Schematic of the enzyme protection against microbiological attack. Enzymes are attached on the carbon film deposited onto the substrate surface and protected by a dense and long carbon nanotube forest. Bacteria cannot reach the protected enzyme molecules. (d), (e) Low- and high-resolution SEM images of *B. subtilis* on the surface of the nanotube pattern after 12 h of incubation. Bacteria were trapped in the upper layer of the nanotube pattern. Reprinted with permission from Kondyurin *et al* [70]. Copyright 2015 Elsevier.

live tissues and cells are now extensively studied including genotoxicity and reproductive toxicity [79], behaviour in live cells [80, 81], applications in cell biology and medicine [82, 83] and other *in vivo* applications [84].

How does the plasma work in this case? A typical process of the silicon nanocrystals fabrication using atmospheric pressure plasmas can be designed as follows [85]. The atmospheric pressure plasma is ignited between the two electrodes by supplying radio frequency power (13.56 MHz). The electrodes are installed in a thin (1 mm dia.) quartz capillary, as shown in figure 9). The plasma-sustaining gas is argon, and silane diluted in argon was used as precursor for the nucleation and growth of silicon nanoparticles. To exclude the contact with ambient air, the whole setup is installed in the metal chamber filled with nitrogen which is supplied to the chamber and then pumped out [86]. This system is simple and convenient in operation, and does not require vacuum pumps.

In the work being discussed [85], the applied RF power was maintained at the level of 100 W, the argon flux was 200 sccm and the argon/silane flux was 50 sccm, with the inter-electrode gap of about 1 mm. The average silane concentration was maintained at the level of 10 ppm. The electric parameters were measured using RF voltage–current probe connected below the matching unit, and at the RF feedthrough outside of the nitrogen-filled chamber.

Importantly, it was demonstrated that the highly crystalline silicon nanoparticles can be nucleated and grown *in atmospheric-pressure low-temperature plasma at temperatures well below the Si crystallization threshold* [85]. These results were interpreted in terms of an efficient heating of the nanoparticles nucleated and growing in non-thermal atmospheric-pressure plasmas. A careful analysis of the energy balance on the surface of plasma-nucleated nanoparticles has revealed that nanocrystals are effectively heated in the atmospheric-pressure plasma.

The two modes of nanoparticle synthesis were compared, and important differences were revealed [85]. Specifically, the energy flux supplied by the ion current to the surfaces of nanoparticle is enhanced in a collisional regime, leading to a higher nanoparticle temperature. In this case the plasma-related effects lead to the low-temperature nucleation, resulting in a better crystalline structure of the nanoparticles.

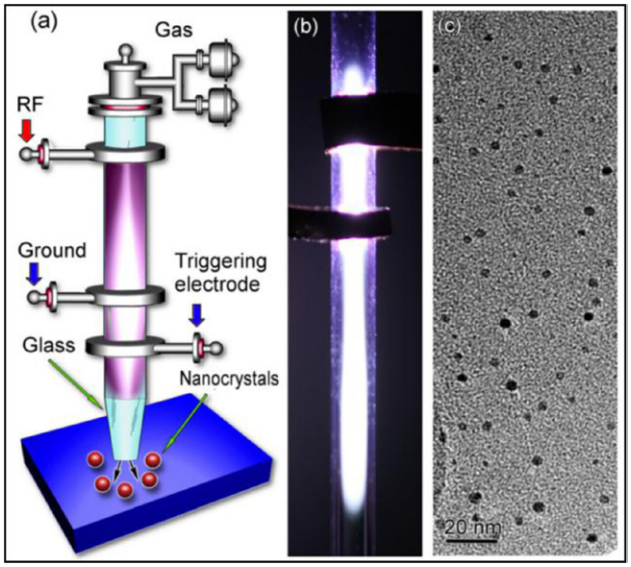

Figure 9. (a) Schematic of the silicon nanoparticles growth in atmospheric plasma jet. (b) Photograph of the plasma jet generated inside a quartz capillary. (c) Representative transmission electron microscopy images of silicon nanoparticles synthesized in the atmospheric-pressure plasma jet. Reprinted with permission from Askari *et al* [85]. Copyright 2014 AIP Publishing.

The *plasma-fabricated and processed Si nanocrystals* were also used to activate nucleation of multiwall carbon nanotubes without any metal catalyst, which can be harmful for the use in living cells or tissues. In these experiments the three different kinds of silicon nanocrystals were used, namely prepared using laser ablation in water and by electrochemical etching and laser fragmentation [87].

For the carbon nanotube growth experiments, the three different types of silicon nanocrystals were first accumulated and stored in water in the form of colloids before the plasma treatment. Just before the plasma processing, the three types of nanocrystal colloids were drop-casted on a silicon wafers and dried in an open air. Then, the dried samples were treated using a microwave plasma-enhanced CVD technique [88]. The sample was first pre-treated in nitrogen plasma at the discharge power of 300 W, pressure of 20 mbar and wafer surface temperature 750 °C. The carbon nanotubes were grown in argon and methane mixture and discharge power of 600 W. The total duration of the nanotube growth process was 5 min.

The results of the carbon nanotube nucleation and growth were different for these different types of nanocrystals (figure 10). Specifically, it was found that the surface features of the nanocrystals are the main factors determining the nucleation and growth of carbon nanotubes. In particular, nanocrystals with a low density of surface oxide have demonstrated more efficient nucleation of nanotubes. Also it was found that the sufficient fragmentation of nanocrystal aggregates into smaller assemblies or even single silicon nanocrystal was also an important factor. In spite of a clear difference observed, the actual mechanism of nanotube nucleation and growth on the silicon nanocrystals is still unknown, and further studies should be conducted to throw light on this problem and deeper understand the *plasma-induced surface processes during nanocrystal functionalization* [89, 90].

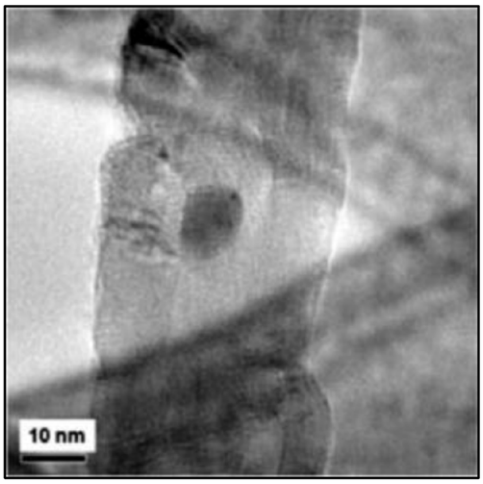

Figure 10. Transmission electron microscopy image showing the presence of silicon nanoparticle within a carbon nanotube. Reprinted with permission from Mariotti *et al* [87]. Copyright 2013 IOP Publishing.

2.5. Hierarchical plasma-treated gold-silver platforms for protein retention

Low temperature plasma treatment can significantly improve the properties of hybrid bioplatforms. Indeed, the reliable surface retention of biologically-active molecules and live cells such as biomolecules [91], stem and red blood cells [92, 93], proteins molecules and biocatalysts [3, 94], various living cells [95], bioethanol-producing bacteria [96] etc. may be useful for various practical applications including biofuel cells [97], food processing techniques [98], biosensors [7], energy conversion and drug delivery devices [1, 99], sensors [100], virus detection [101], microfluidic devices [102], fluidised bed bioreactors [5], fixed-bed catalytic reactors [103] and many others. Various metamaterials and nanoscaled systems such as mesoporous carbon beads [104], nanostructured polymer surfaces [105], silica/polymer matrices [106] and nanoporous membranes [107] with the nanometre-scale morphology for enhancing protein adsorption [108] were proposed in the capacity of a supporting platform. It was demonstrated recently that the hierarchical structures utilising vertically-aligned carbon nanotubes [70, 109] and patterns of vertically-aligned carbon nanowalls [110] also can be used as biotechnological nano-structured platforms.

The structures comprising nanostructures made of noble metals are especially promising due to their chemical inertness, as well as absence of carbon-containing and other complex organic contaminations. This requirement is of importance for bio- and medical applications [111] including precise diagnostics [112]. Moreover, such materials allow for the fast and convenient deactivation and sterilization.

Among other combinations, the platforms comprising gold base and patterns of vertically-aligned 1D silver nanostructures (i.e. nanowires) have recently attracted major attention [113]. 1D nanostructures (nanocones, nanofibers, nanowires and others) are used in some specific applications such as nanoelectronics [114] and energy storage and conversion

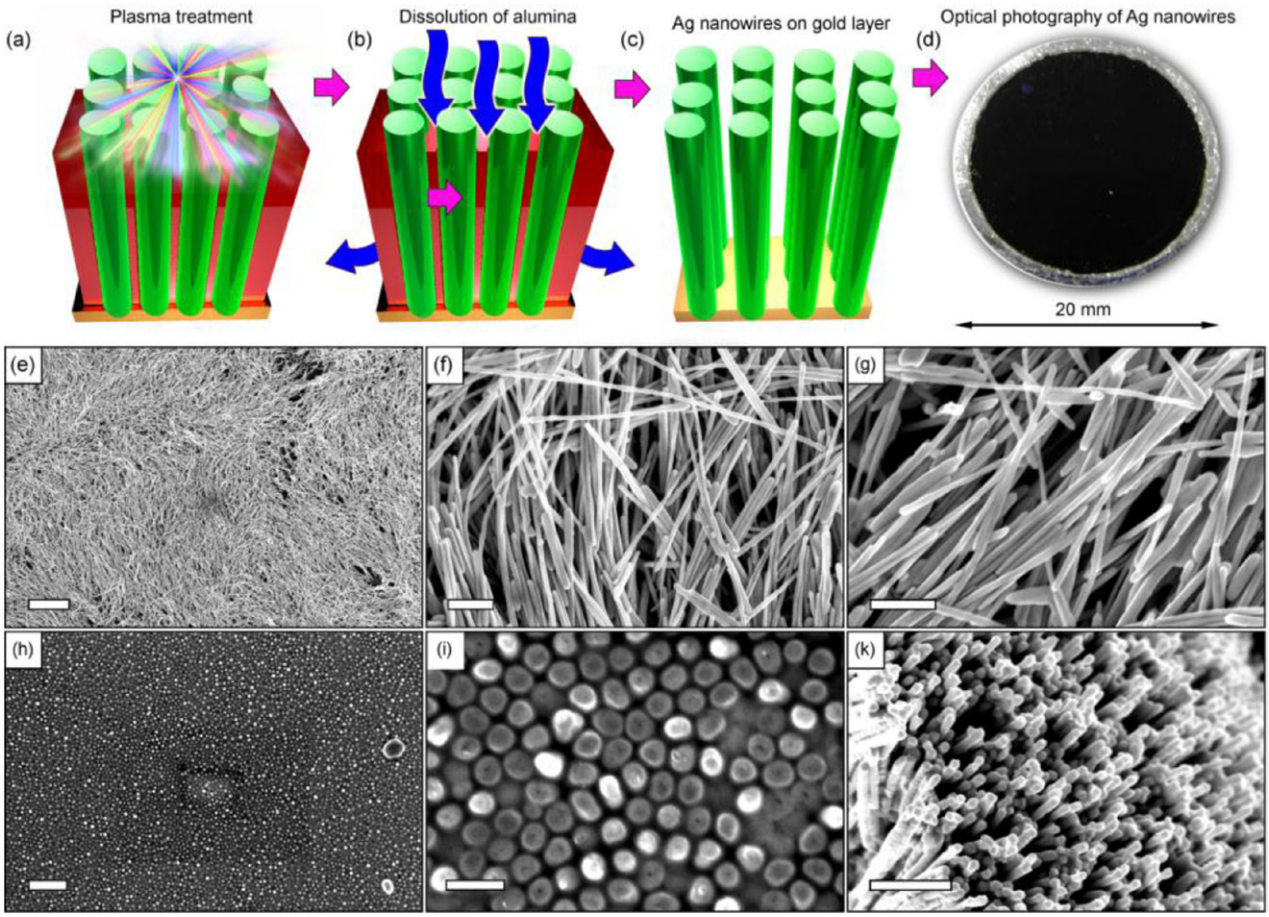

Figure 11. Fabrication of the platform with silver nanowires, and scanning electron microscopy images of the nanowires. Plasma treatment of nanowires (a); dissolution of aluminum oxide in acid (b), and 3D model of the ready platform (c). (d) Optical photography of the Ag nanowires, top view. (e)–(g) Low- and high-magnification scanning electron microscopy images of silver nanowires after dissolution of the membrane, without the plasma treatment. The length of nanowires reached several tens of μm. Scale bars are 10 μm (e) and 500 nm (f), (g). (h)–(k) Low- and high-magnification scanning electron microscopy images of silver nanowires after dissolution of the membrane in acid and the plasma treatment. The nanowires are much shorter after the plasma treatment, as seen from thecomparison of panels (g) and (k). Scale bars are 1 μm (h) and 500 nm (i), (k). Reprinted with permission from Fang *et al* [133].

devices [115]. It is known that silver exhibits strong antimicrobial activity, strongest when silver is present in the form of nanowires [116], nanoparticles [117, 118], and complex nanoarchitectures involving silver and gold nanostructures [119]. Moreover, gold nanostructures are suitable for retention of biological molecules [120].

Based on this analysis, several successful attempts were made to build nanoplatforms incorporating silver nanowires. In one of the successful experiments (figure 11), a large dense pattern of silver nanowires was grown on the nanoporous aluminium oxide membrane. The grown pattern was dense enough to ensure small gaps between the nanowires and hence, efficient protection from the microbiological attacks (see section 2.3). Specifically, the gaps did not exceed several hundred nanometres and thus made the bottom of the platform not accessible for most bacteria which have a size reaching one to several micrometres.

What is the plasma role in this case? The low-temperature plasma treatment was used to control the structure, state, and morphology of the silver nanowire pattern due to the plasma-specific effects, i.e. bombardment of the nanostructures by energetic ions accelerated across the plasma bulk—surface electric field. Besides, the ability of the platform to retain the proteins at the bottom layers, i.e. where they are protected from the effect of live bacteria, was also controlled by the plasma treatment.

The samples were treated with the atmospheric-pressure plasma jet, i.e. the vacuum and gas-containing chambers were not used in this case. More information about the discharge, design of the plasma generating reactor, and plasma treatment can be found elsewhere [85, 121]. The treated samples were then tested for the ability to capture and immobilize the proteins. The commonly used Bovine Serum Albumin was used in these experiments, to avoid contamination. This protein is cheap and commonly available, and can be used as a reference in many experiments including ELISA.

The conducted experiments have demonstrated that the atmospheric-pressure plasma treatment (as well as processing with the low-temperature inductively coupled plasmas) indeed can be helpful in controlling the structure and morphology of the hybrid platforms, and importantly, can control the ability of retaining active protein molecules and other species. Specifically, it was demonstrated that the *amount of retained protein may be increased due to the plasma-related effects.*

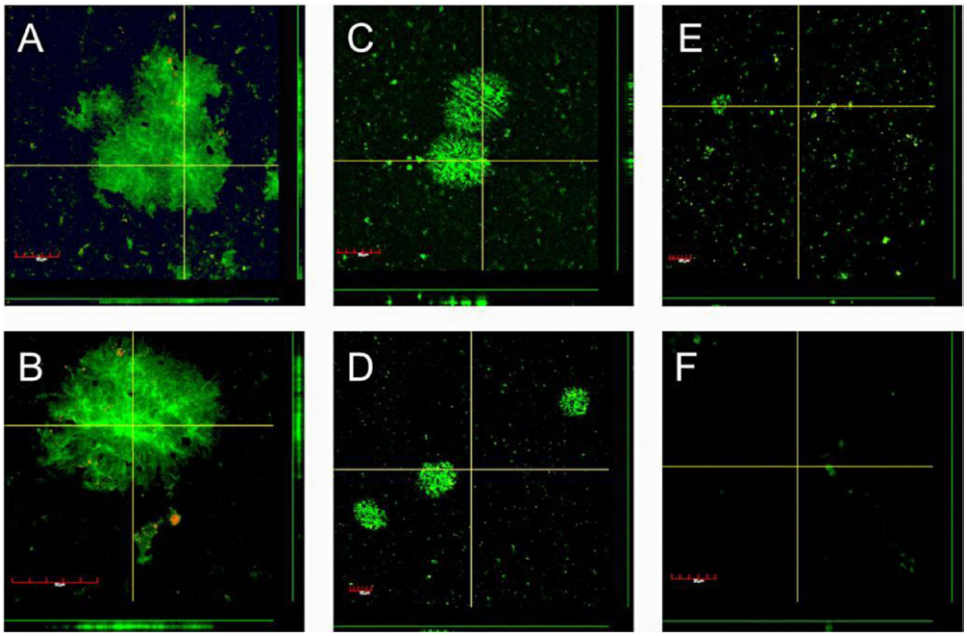

Figure 12. Confocal images of *P. aeruginosa* biofilms cells after argon plasma treatment stained with Bac Light Live/Dead. Viable cells are stained green and dead cells are stained red (A) Untreated control, (B) 10 min argon gas control, (C) 1 min plasma, (D) 3 min plasma, (E) 5 min plasma and (F) 10 min plasma treatment. Each image shows a representative horizontal section (main picture), and two vertical sections (to the right of and below the green lines on the right-hand side and bottom of the main picture, respectively). The vertical sections correspond to the two yellow lines in the main picture. Reprinted with permission from Mai-Prochnow *et al* [135].

We should stress here that the alloyed nanostructures, as well as nanostructures with complex chemical composition are not discussed in much detail in this review, which is mainly dealing with the plasma-related effects. The processes in plasma environment consisting of many compounds (e.g. when plasma is sustained in the mixture of reagent gases) have very complex nature, and the interested reader should refer to the topical publications. Nevertheless, the alloyed nanostructures are among the most important plasma-made nanoscaled materials, and thus we will list here several typical examples. Among many others, the following examples could be indicated. Fabrication of hydroxyapatite bioceramics on TiAlV orthopaedic alloys for biomedical applications [122] is an excellent example when plasma enabled creation of complex alloyed nanostructure. Alloyed Au_xAg_{1-x} nanoparticles [123] made via microplasma-chemical synthesis for the applications requiring tunable real-time plasmonic responses is one more typical example. The amorphous silicon quantum dots were also prepared by plasma hydrogenation [124]. More details on the atmospheric pressure plasma-enabled synthesis and composition tuning of complex alloyed nanostructures could be found in the topical review [86].

3. Plasma—a tool for treatment and functionalization

Here we will examine two examples of the plasma application for the surface functionalization and direct activation. Specifically, we consider the control of carbon nanotube arrays biocompatibility by plasma post-processing, and direct effect of the low-temperature plasmas onto living cells.

3.1. Plasma treatment of carbon nanotube arrays to control growth of bacterial biofilms

We have discussed the possibility to control the viability of the cultivated bacteria on plasma-treated nanostructures (see section 2.3 above), but another interesting question is the control of bacterial biofilm formation.

3.1.1. Can the plasma treatment control the biofilm formation?

Several studies have shown that carbon nanotubes have antibacterial properties (see section 2.3). However, most of these studies focus on dispersed nanotubes interactions with free living (planktonic) bacteria, rather than the most prevalent bacterial growth form—biofilms. Biofilm cells live in a multi-layer community enclosed by an extracellular matrix [125]. This lifestyle offers bacteria higher protection from external stresses and thus can lead to problems of eradicating unwanted biofilms. While some bacterial biofilms can be useful for waste water treatment [126, 127], starch hydrolysis [128], microbial fuel cells [5, 129] and antifouling coatings [130, 131] others are harmful, fouling films or pathogens causing hard to treat infections [132].

The effects of nanotube arrays on bacteria of different species have recently been investigated [68]. It was found that unlike dispersed nanotubes they exhibit only mild antibacterial effect and thus their biocompatibility is higher. Nanotube arrays treated with inductively coupled plasma retained morphological integrity of the nanostructure, in particular in the presence of bacteria and their liquid growth media. Bacteria stayed on top of the arrays and cannot penetrate through the structure. Both Gram positive (*B. subtilis*) and Gram negative (*E. coli*) bacteria were tested for survival in the presence of nanotube arrays. Interestingly, only *B. subtilis* seemed to be

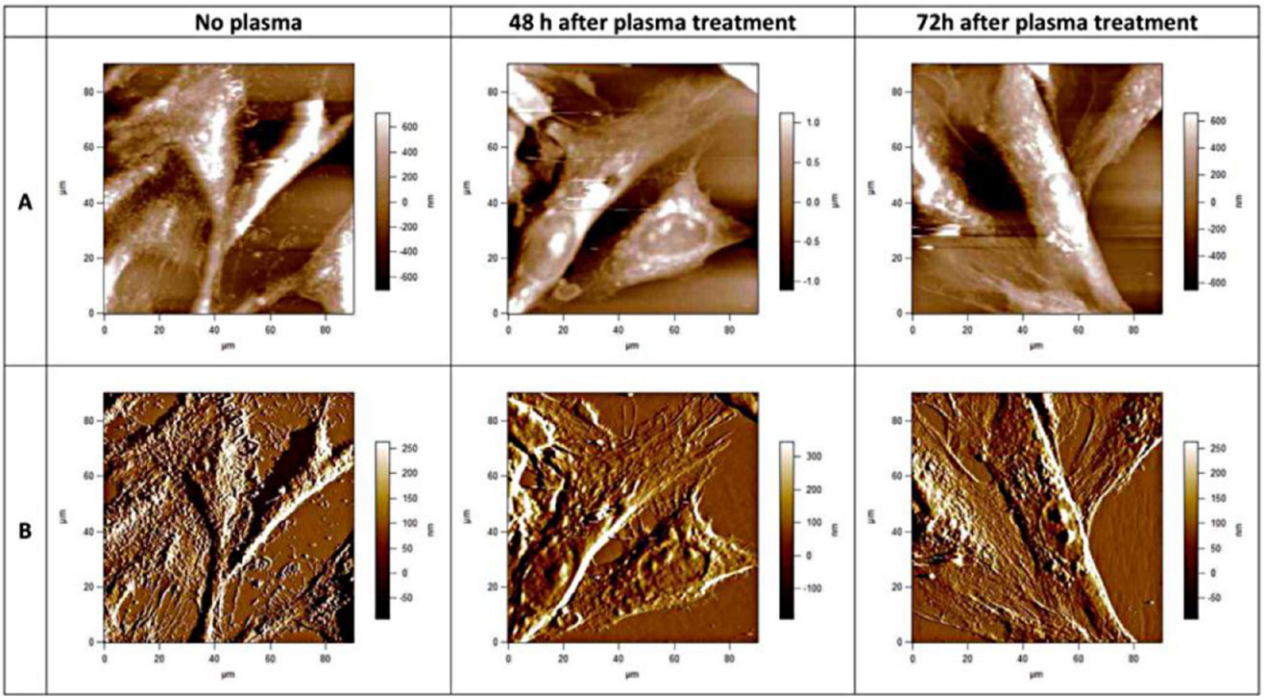

Figure 13. AFM images of fixed NHA (E6/E7), taken using the Igor Pro 4 software, 90 × 90 μm scans. Upper row (A), topographies of 2D images of E6/E7 cells before and 48 h and 72 h after the plasma treatment; lower row (B), corresponding deflection signal images. Cells were treated with cold plasma for 30 s. All images presented here were obtained in a contact mode at room temperature and scanned in PBS. Reprinted with permission from Recek *et al* [156].

inhibited by pristine arrays but not by the plasma functionalized nanotubes.

Investigation on how plasma treatment affects surface attached bacteria has implications for the use of biomaterials, such as medical implants [133]. Moreover, these studies are important for deeper understanding the processes occurring during the plasma effects on the bacterial biofilms. Commonly, three antibacterial methods for carbon nanotubes were reported: (1) oxidative stress, (2) metal toxicity and (3) mechanical piercing [134]. It was suggested that plasma assisted functionalising of carbon nanotubes may scavenge free radicals and lead to less bacterial inhibition of the functionalised samples [68]. Furthermore, it was proposed that by functionalising nanotube arrays the hydrophobicity is increased, reducing the piercing ability. It can be concluded that plasma-assisted functionalising of the carbon nanotube arrays leads to higher biocompatibility.

In another relevant study, the behaviour of bacterial biofilms on stainless steel coupons was studied [135]. The direct effect of the plasma treatment on surface attached bacterial communities was investigated using the antibiotic-resistant bacterium *P. aeruginosa* as a model organism to determine whether cells can develop resistance to the plasma treatment. Biofilms on stainless steel coupons could be completely removed by 10 min argon plasma treatment (figure 12). Because of the multi-factorial action of plasma on living cells (reactive oxygen and nitrogen species (RONS), UV, and excited molecules) it is widely assumed that bacterial cells are unlikely to develop a resistance to the plasma treatment as seen with many antibiotics. However, in the study being discussed some bacteria were shown to survive a shorter plasma treatment and then exhibit a higher resistance to subsequent treatments. These cells had permanent genetic changes. In the case of *P. aeruginosa* it is a redox active compound phenazine [135].

3.2. Toxicity of nanoparticles and nanocomposites—effect of treatment, outer coatings, and material

The toxicity of nanoparticles, nanomaterials and various surface-based nanostructures and nanosystems is one more important issue that could be affected by plasma treatment and other surface processes, including application of thin coatings to the nanoparticles and surface-active treatment [136]. Even gold nanoparticles should be considered as a nanosystem requiring specific considerations in relation to the toxicity in particular conditions and environment [137], and their toxicity depends on the physiochemical properties and size [138].

Material toxicity can be affected by many routes, and surface coating and modification are among the most efficient techniques for nanoscaled particles. Indeed, the toxicity of iron oxide nanoparticles (important system for medical applications) could be tuned by, e.g. silica (silicon oxide) coating, as confirmed by *in vitro* studies [139]. Toxicity of silver nanoparticles essentially depends of their size and surface state, and surface coating (e.g. using polyvinylpyrrolidone) could significantly change the toxicity level [140]. Cytotoxicity of silver nanocrystallites also could be tuned by surface coatings [141]. Carbon films could be used to tune the toxicity characteristics of iron oxide nanoparticles [142].

Toxicity of graphene fragment is also an issue, and plasma treatment could be a good solution in this case (provided that

the graphene-specific properties are not disturbed by the treatment) [143, 144]. On the other hand, nanoscaled particles could have quite attractive clinical potential [145, 146], even when they possess toxic properties. Plasma and chemical modification of surface structures and properties of the nanoscaled carbonous materials is also quite promising approach [147].

Toxicity and biological activity of carbon nanotubes and nanowires, owing to their small diameter and often acute ends, is also an issue [148]. In this case, plasma could be used to modify the shape and state (open/closed tips) of the nanotube arrays, and thus the toxicity and biological activity could be controlled along with other important properties such as wettability [70, 149].

3.3. Direct effect of low-temperature plasma on living cells

To deeper understand the plasma effect onto biomaterials and optimize the processes of biomaterial fabrication and functionalization, the direct effect of plasma streams onto living cells should be studied. Besides, such studies are important for some hard-pressing medical problems such as cancer treatment by direct plasma effect onto cells [150–152] and via the nanostructures [153], as well as for other medical applications such as electric surgery [154, 155]. These and other publications represent a good deal of accumulated data on the effect of plasma onto living cell; we will here briefly examine only one typical example.

Specifically, the selective effect of cold plasma on shape and morphology of normal human astrocytes (NHA) and glioblastoma cells was the aim of the research [156]. The atomic force microscopy (AFM) technique has been used to image the cells *before and after the plasma treatment* (figure 13).

In these experiments, a cold plasma jet was used [157]. It consists of a central electrode installed in the glass tube, and the second electrode placed outside. A pulsed voltage was applied to the central electrode, whereas the outside electrode was grounded. Helium gas was supplied to the glass tube to sustain the discharge and produce the plasma jet. The experiments were mainly aimed to study the selective effect of cold plasma jet treatment on shape and morphology of the fixed NHA and glioblastoma cells. The cell viability was assessed using a standard colorimetric assay for measuring the activity of mitochondria and cellular dehydrogenase enzymes.

Both NHA E6/E7 and glioblastoma U87 cells were processed with the cold plasma jet for various time durations. The results of the MTT assay characterization have shown that a significant part of U87 cells died after the short processing, whereas from 90 to 60% of E6/E7 cells have retained the viability. Repeated experiments and comparison with the reference cultures have demonstrated that the 30 s treatment is a threshold duration required for the significant decrease of viability. More details on the experiments and obtained results can be found elsewhere [156].

The morphological features on U87 and E6/E7 cells were then studied using the AFM technique. The AFM studies were conducted in a contact mode by acquiring the height of contours, and surface morphology by the deflection signal. Figure 13(a) shows the topographical parameters of complete E6/E7 cell, and figure 13(b) presents the corresponding deflection image. The information in the topography image (figure 13(a)) is dominated by the nucleus, although other features, such as the cell boundaries and the microvilli or invadopodia can be clearly distinguished. The untreated U87 and E6/E7 cells are extensively spread; cell body, shape, morphology, microvilli and invadopodia were clearly visible on the AFM images. The position of the cell bodies can be seen as well as where the cells meet (figure 13). Large fibre structures were seen on images of both U87 and E6/E7 adherent cells, although they were more pronounced on E6/E7 cells (figure 13).

The experiments with plasma treated fixed cells bring to the light new important understanding of the architecture and assembly of the cell membrane in NHA and glioblastoma cells. They also contribute to the understanding the complex interaction between the plasma and the cell membrane surface. These differences could be the possible reason for the *selective effect of plasma on glioblastoma cells* and may significantly contribute to *cell viability after the plasma treatment*.

4. Concluding remarks

In this review, we have briefly examined various approaches based on the use of low-temperature plasmas to fabricate nanostructured biomaterials and systems exhibiting biological activity for medical treatment, biological inertness for drug delivery system, and other features that make them attractive. In particular, we have discussed the plasma-assisted fabrication of gold and silicon nanoparticles for bio-applications; atmospheric-pressure plasma fabrication of carbon nanoparticles for bioimaging and cancer therapy; plasma-activated carbon nanotube-based platforms for enzyme production and bacteria growth control, and other applications of low-temperature plasmas in the production of biologically-active materials. In the considered cases the effect of low-temperature plasmas have led to better results, as compared with the conventional neutral-gas based techniques.

Acknowledgments

IL acknowledges the support from the School of Chemistry, Physics and Mechanical Engineering, Science and Engineering Faculty, Queensland University of Technology. This work was partially supported by the Australian Research Council and CSIRO's OCE Science Leadership Scheme, and partially supported by Slovenian Research Agency (ARRS), project L2-6769.

References

[1] Schoonen L and van Hest J C 2014 Functionalization of protein-based nanocages for drug delivery applications *Nanoscale* **6** 7124–41
[2] Martinho N, Damgé C and Reis C P 2011 Recent advances in drug delivery systems *J. Biomater. Nanobiotechnol.* **2** 510–26
[3] Bilek M M M 2014 Biofunctionalization of surfaces by energetic ion implantation: review of progress on

applications in implantable biomedical devices and antibody microarrays *Appl. Surf. Sci.* **310** 3–10
[4] Regil R and Sandoval G 2013 Biocatalysis for biobased chemicals *Biomolecules* **3** 812–47
[5] Godia F and Sola C 1995 Fluidized bed bioreactors *Biotechnol. Prog.* **11** 479–97
[6] Gilbert E, Mosher M, Gottipati A and Elder S 2014 A novel through-thickness perfusion bioreactor for the generation of scaffold-free tissue engineered cartilage *Processes* **2** 658–74
[7] Wanekaya A K, Chen W, Myung N V and Mulchandani A 2006 Nanowire-based electrochemical biosensors *Electroanalysis* **18** 533–50
[8] Arnold M A and Meyerhoff M E 1988 Recent advances in the development and analytical applications of biosensing probes *Crit. Rev. Anal. Chem.* **20** 149–96
[9] Havard H and Miles J 2015 Biofilm and orthopaedic implant infection *J. Trauma Orthop.* **03** 54–7
[10] Wesley M J, Lerner R N, Kim E S, Islam M D S and Liu Y 2011 Biological fixed film *Water Environ. Res.* **83** 1150–86
[11] Levchenko I *et al* 2015 Hybrid carbon-based nanostructured platforms for the advanced bioreactors *J. Nanosci. Nanotechnol.* **15** 10074–90
[12] Levchenko I, Keidar M, Mai-Prochnow A, Modic M, Cvelbar U, Fang J and Ostrikov K 2015 Plasma treatment for next-generation nanobiointerfaces *Biointerphases* **10** 029405
[13] Tang L, Wang Y and Li J 2015 The graphene/nucleic acid nanobiointerface *Chem. Soc. Rev.* **44** 6954–80
[14] Gu X, Zheng Y, Cheng Y, Zhong S and Xi T 2009 *In vitro* corrosionand biocompatibility of binary magnesium alloys *Biomaterials* **30** 484–98
[15] Nichols S P, Koh A, Storm W L, Shin J H and Schoenfisch M H 2013 Biocompatible materials for continuous glucose monitoring devices *Chem. Rev.* **113** 2528–49
[16] Tie D, Feyerabend F, Müller W D, Schade R, Liefeith K, Kainer K U and Willumeit R 2013 Antibacterial biodegradable Mg–Ag alloys *Eur. Cells Mater.* **25** 284–98
[17] Dolanský J, Henke P, Kubát P, Fraix A, Sortino S and Mosinger J 2015 Polystyrene nanofiber materials for visible-light-driven dual antibacterial action via simultaneous photogeneration of NO and $O_2(1\Delta g)$ *ACS Appl. Mater. Interfaces* **7** 22980–9
[18] Levchenko I, Romanov M and Keidar M 2003 Investigation of a steady-state cylindrical magnetron discharge for plasma immersion treatment *J. Appl. Phys.* **94** 1408–13
[19] Levchenko I, Keidar M, Xu S, Kersten H and Ostrikov K 2013 Low-temperature plasmas in carbon nanostructure synthesis *J. Vac. Sci. Technol.* B **31** 050801
[20] Chu P K 2007 Plasma-treated biomaterials *IEEE Trans. Plasma Sci.* **35** 181–7
[21] Ostrikov K, Cvelbar U and Murphy A B 2011 Plasma nanoscience: setting directions, tackling grand challenges *J. Phys. D: Appl. Phys.* **44** 174001
[22] Jain S, Hirst D G and O'Sullivan J M 2012 Gold nanoparticles as novel agents for cancer therapy *Br. J. Radiol.* **85** 101–13
[23] Kodiha M, Wang Y M, Hutter E, Maysinger D and Stochaj U 2015 Off to the organelles—killing cancer cells with targeted gold nanoparticles *Theranostics* **5** 357–70
[24] Anker J N, Hall W P, Lyandres O, Shah N C, Zhao J and van Duyne R P 2008 Biosensing with plasmonic nanosensors *Nat. Mater.* **7** 442–53
[25] Pengo P, Baltzer L, Pasquato L and Scrimin P 2007 Substrate modulation of the activity of an artificial nanoesterase made of peptide-functionalized gold nanoparticles *Angew. Chem. Int. Ed.* **46** 400–6
[26] Lhoste K, Malaquin L, Billot L, Haghiri-Gosnet A M and Chen Y 2011 Fabrication of high density gold nanoparticle arrays on glass for high sensitivity bio-detection *Microelectron. Eng.* **88** 2474–7
[27] Phuc T D, Yoshino M, Yamanaka A and Yamamoto T 2013 Fabrication of gold nanodot array on plastic films for bio-sensing applications *Proc. CIRP* **5** 47–52
[28] Willner I, Baron R and Willner B 2007 Integrated nanoparticle-biomolecule systems for biosensing and bioelectronics *Biosens. Bioelectron.* **22** 1841–52
[29] Ostrikov K and Mehdipour H 2012 Nanoscale plasma chemistry enables fast, size-selective nanotube nucleation *J. Am. Chem. Soc.* **134** 4303–12
[30] Ding H, Yong K-T, Roy I, Pudavar H E, Law W C, Bergey E J and Prasad P N 2007 Gold nanorods coated with multilayer polyelectrolyte as contrast agents for multimodal imaging *J. Phys. Chem.* C **111** 12552–7
[31] Miyanishi T, Tsunoi Y, Terakawa M and Obara M 2012 High-intensity near-field generation for silicon nanoparticle arrays with oblique irradiation for large-area high-throughput nanopatterning *Appl. Phys.* B **107** 323–32
[32] Whitney A V, Elam J W, Zou S, Zinovev A V, Stair P C, Schatz G C and van Duyne R P 2005 Localized surface plasmon resonance nanosensor: a high-resolution distance-dependence study using atomic layer deposition *J. Phys. Chem.* B **109** 20522–8
[33] Yajadda M M A, Levchenko I and Ostrikov K 2011 Gold nanoresistors with near-constant resistivity in the cryogenic-to-room temperature range *J. Appl. Phys.* **110** 023303
[34] Levchenko I, Kumar S, Yajadda M M A, Han Z J, Furman S and Ostrikov K 2011 Self-organization in arrays of surface-grown nanoparticles: characterization, control, driving forces *J. Phys. D: Appl. Phys.* **44** 174020
[35] Xu S, Huang S Y, Levchenko I, Zhou H P, Wei D Y, Xiao S Q, Xu L X, Yan W S and Ostrikov K 2011 Highly efficient silicon nanoarray solar cells by a single-step plasma-based process *Adv. Energy Mat.* **1** 373–6
[36] Levchenko I, Ostrikov K, Rider A E, Tam E, Vladimirov S V and Xu S 2007 Growth kinetics of carbon nanowall-like structures in low-temperature plasmas *Phys. Plasmas* **14** 063502
[37] Levchenko I, Korobov M, Romanov M and Keidar M 2004 Ion current distribution on a substrate during nanostructure formation *J. Phys. D: Appl. Phys.* **37** 1690–5
[38] Levchenko I, Ostrikov K, Mariotti D and Švrček V 2009 Self-organized carbon connections between catalyst particles on a silicon surface exposed to atmospheric-pressure Ar + CH_4 microplasmas *Carbon* **47** 2379–90
[39] Cvelbar U, Ostrikov K, Levchenko I, Mozetic M and Sunkara M K 2009 Control of morphology and nucleation density of iron oxide nanostructures by electric conditions on iron surfaces exposed to reactive oxygen plasmas *Appl. Phys. Lett.* **94** 211502
[40] Levchenko I, Ostrikov K and Mariotti D 2009 The production of self-organized carbon connections between Ag nanoparticles using atmospheric microplasma synthesis *Carbon* **47** 344–7
[41] Levchenko I, Ostrikov K and Long J D 2007 Plasma-assisted self-sharpening of platelet-structured single-crystalline carbon nanocones *Appl. Phys. Lett.* **91** 113115
[42] Keidar M, Beilis I I, Boxman R L and Goldsmith S 1996 2D expansion of the low-density interelectrode vacuum arc plasma jet in an axial magnetic field *J. Phys. D: Appl. Phys.* **29** 1973
[43] Tsakadze Z L, Levchenko I, Ostrikov K and Xu S 2007 Plasma-assisted self-organized growth of uniform carbon nanocone arrays *Carbon* **45** 2022
[44] Ray S C, Saha A, Jana N R and Sarkar R 2009 Fluorescent carbon nanoparticles: synthesis, characterization, and bioimaging application *J. Phys. Chem.* C **113** 18546–51
[45] Liu Z and Liang X J 2012 Nano-carbons as theranostics *Theranostics* **2** 235

[46] Kharin A, Syshchyk O, Geloen A, Alekseev S, Rogov A, Lysenko V and Timoshenko V 2015 Carbon fluoroxide nanoparticles as fluorescent labels and sonosensitizers for theranostic applications *Sci. Technol. Adv. Mater.* **16** 044601

[47] Kumar V, Toffoli G and Rizzolio F 2013 Fluorescent carbon nanoparticles in medicine for cancer therapy *ACS Med. Chem. Lett.* **4** 1012–13

[48] Liu R, Wu D, Liu S, Koynov K, Knoll W and Li Q 2009 An aqueous route to multicolor photoluminescent carbon dots using silica spheres as carriers *Angew. Chem. Int. Ed. Engl.* **48** 4598–601

[49] Hong G, Diao S, Antaris A L and Dai H 2015 Carbon nanomaterials for biological imaging and nanomedicinal therapy *Chem. Rev.* **115** 10816–906

[50] Bogaerts A, Khosravian N, van der Paal J, Verlackt C C W, Yusupov M, Kamaraj B and Neyts E C 2016 Multi-level molecular modelling for plasma medicine *J. Phys. D: Appl. Phys.* **49** 054002

[51] Hundt M, Sadler P, Levchenko I, Wolter M, Kersten H and Ostrikov K 2011 Real-time monitoring of nucleation-growth cycle of carbon nanoparticles in acetylene plasmas *J. Appl. Phys.* **109** 123305

[52] Ketelsen H 2009 Mie-ellipsometrie an staubigen plasmen *Dipl. Eng. PhD Thesis* University of Kiel, Germany

[53] Kabbadj Y, Herman M, Lombardi G D, Fusina L and Johns J W 1991 *J. Mol. Spectrosc.* **150** 535–47

[54] Rothmann L 2009 HITRAN Database URL www.cfa.harvard.edu/hitran

[55] Watanabe Y 2006 Formation and behaviour of nano/micro-particles in low pressure plasmas *J. Phys. D: Appl. Phys.* **39** R329

[56] Cui C and Goree J 1994 Fluctuations of the charge on a dust grain in a plasma *IEEE Trans. Plasma Sci.* **22** 151–8

[57] Mankelevich Y A, Olevanov M A and Rakhimova T V 2008 Dust particle coagulation mechanism in low-pressure plasma: rapid growth and saturation stage modeling *Plasma Sources Sci. Technol.* **17** 015013

[58] Mankelevich Y, Olevanov M, Pal' A, Rakhimova T, Ryabinkin A, Serov A and Filippov A 2009 Coagulation of dust grains in the plasma of an RF discharge in argon *Plasma Phys. Rep.* **35** 191–9

[59] Hollenstein Ch 2000 The physics and chemistry of dusty plasmas *Plasma Phys. Control. Fusion* **42** R93–104

[60] Levchenko I, Ostrikov K, Zheng J, Li X, Keidar M and Teo K 2016 Scalable graphene production: perspectives and challenges of plasma applications *Nanoscale* **8** 10511–27

[61] Keidar M, Levchenko I, Arbel T, Alexander M, Waas A M and Ostrikov K 2008 Magnetic-field-enhanced synthesis of single-wall carbon nanotubes in arc discharge *J. Appl. Phys.* **103** 094318

[62] Keidar M, Raitses Y, Knapp A and Waas A M 2006 Current-driven ignition of single-wall carbon nanotubes *Carbon* **44** 1022–4

[63] Sun X, Li R, Stansfield B, Dodelet J P, Menard G and Desilets S 2007 Controlled synthesis of pointed carbon nanotubes *Carbon* **45** 732–7

[64] Burian A, Dore J C, Kyotani T and Honkimaki V 2005 Structural studies of oriented carbon nanotubes in alumina channels using high energy x-ray diffraction *Carbon* **43** 2723–9

[65] Shim M, Kam N W S, Chen R J, Li Y and Dai H 2002 Functionalization of carbon nanotubes for biocompatibility and biomolecular recognition *Nano Lett.* **2** 285–8

[66] Fisher C, Rider A E, Han Z J, Kumar S, Levchenko I and Ostrikov K 2012 Applications and nanotoxicity of carbon nanotubes and graphene in biomedicine *J. Nanomater.* **2012** 315185

[67] Peng X and Wong S S 2009 Functional covalent chemistry of carbon nanotube surfaces *Adv. Mater.* **21** 625–42

[68] Yick S, Mai-Prochnow A, Levchenko I, Fang J, Bull M K, Bradbury M, Murphy A B and Ostrikov K 2015 The effects of plasma treatment on bacterial biofilm formation on vertically-aligned carbon nanotube arrays *RSC Adv.* **5** 5142

[69] Levchenko I, Romanov M, Keidar M and Beilis I I 2004 Stable plasma configurations in a cylindrical magnetron discharge *Appl. Phys. Lett.* **85** 2202–4

[70] Kondyurin A, Levchenko I, Han Z, Yick S, Mai-Prochnow A, Fang J, Ostrikov K and Bilek M 2013 Hybrid graphite film-carbon nanotube platform for enzyme immobilization and protection *Carbon* **65** 287–95

[71] Erogbogbo F, Yong K T, Roy I, Xu G X, Prasad P and Swihart M T 2008 Biocompatible luminescent silicon quantum dots for imaging of cancer cells *ACS Nano* **5** 873–8

[72] Timoshenko V Y, Kudryavtsev A A, Osminkina L A, Vorontsov A S, Ryabchikov Y V, Belogorokhov I A, Kovalev D and Kashkarov P K 2006 Silicon nanocrystals as photosensitizers of active oxygen for biomedical applications *JETP Lett.* **83** 423–6

[73] Kovalev D and Fujii M 2005 Silicon nanocrystals: photo-sensitizers for oxygen molecules *Adv. Mat.* **17** 2531–44

[74] Borsella E, Falconieri M, Herlin N, Loschenov V, Miserocchi G, Nie Y, Rivolta I, Ryabova A and Wang D 2010 *Biomedical and Sensor Applications of Silicon Nanoparticles, in Silicon Nanocrystals: Fundamentals, Synthesis and Applications* ed L Pavesi and R Turan (Weinheim: Wiley-VCH)

[75] Nishimura H *et al* 2013 Biocompatible fluorescent silicon nanocrystals for single-molecule tracking and fluorescence imaging *J. Cell Biol.* **202** 967–83

[76] Medintz I L, Uyeda H T, Goldman E R and Mattoussi H 2005 Quantum dot bioconjugates for imaging, labelling and sensing *Nat. Mater.* **4** 435–46

[77] Cheng A, Decuzzi P, Tour J M, Robertson F and Ferrari M 2008 Mesoporours silicon particles as a multistage delivery system for imaging and therapeutic applications *Nat. Nanotechnol.* **3** 151–7

[78] Canham L T 2007 Nanoscale semiconducting silicon as a nutritional food additive *Nanotechnology* **18** 1–6

[79] Durnev A D *et al* 2010 Evaluation of genotoxicity and reproductive toxicity of silicon nanocrystal *Bull Exp. Biol. Med.* **149** 445–9

[80] Fucikova A, Valenta J, Pelant I, Kalbacova M, Broz A, Rezek B, Kromka A and Bakaeva Z 2014 Silicon nanocrystals and nanodiamonds in live cells: photoluminescence characteris-tics, cytotoxicity and interaction with cell cytoskeleton *RSC Adv.* **4** 10334–42

[81] Jaiswal J K and Simon S M 2004 Potentials and pitfalls of fluorescent quantum dots for biological imaging *Trends Cell Biol.* **14** 497–504

[82] O'Farrell N, Houlton A and Horrocks B R 2006 Silicon nanoparticles: applications in cell biology and medicine *Int. J. Nanomed.* **1** 451–72

[83] Fucikova A, Valenta J, Pelant I and Brezina V 2009 Novel use of silicon nanocrystals and nanodiamonds in biology *Chem. Papers* **63** 704–8

[84] Park J H, Gu L, von Maltzahn G, Ruoslahti E, Bhatia S N and Sailor M J 2009 Biodegradable luminescent porous silicon nanoparticles for *in vivo* applications *Nat. Mater.* **8** 331–6

[85] Askari S, Levchenko I, Ostrikov K, Maguire P and Mariotti D 2014 Crystalline Si nanoparticles below crystallization threshold: effects of collisional heating in non-thermal atmospheric-pressure microplasmas *Appl. Phys. Lett.* **104** 163103

[86] Askari S, Macias-Montero M, Velusamy T, Maguire P, Svrcek V and Mariotti D 2015 Silicon-based quantum dots: synthesis, surface and composition tuning with atmospheric pressure plasmas *J. Phys. D: Appl. Phys.* **48** 314002

[87] Mariotti D, Svrcek V, Mathur A, Dickinson C, Matsubara K and Kondo M 2013 Carbon nanotube growth activated by quantum-confined silicon nanocrystals *J. Phys. D: Appl. Phys.* **46** 122001

[88] Mathur A, Roy S S, Tweedie M, Maguire P D and McLaughlin J A 2009 Electrical and Raman spectroscopic studies of vertically aligned multi-walled carbon nanotubes *J. Nanosci. Nanotechnol.* **9** 4392–6

[89] Mariotti D, Patel J, Svrcek V and Maguire P 2012 Plasma–liquid interactions at atmospheric pressure for nanomaterials synthesis and surface engineering *Plasma Proc. Polym.* **9** 1074–85

[90] Thanh N T K and Green L A W 2010 Functionalisation of nanoparticles for biomedical applications *Nano Today* **5** 213–30

[91] Vashist S K, Schneider E M, Lam E, Hrapovic S and Luong J H T 2014 One-step antibody immobilization-based rapid and highly-sensitive sandwich ELISA procedure for potential *in vitro* diagnostics *Sci. Rep.* **4** 4407–12

[92] Ribaut C, Reybier K, Torbiero B, Launay J, Valentin A, Reynes O, Fabre P L and Nepveu F 2008 Strategy of red blood cells immobilisation onto a gold electrode: characterization by electrochemical impedance spectroscopy and quartz crystal microbalance *IRBM* **29** 141–8

[93] Wang M, Castro N J, Li J, Keidar M and Zhang L G 2012 Greater osteoblast and mesenchymal stem cell adhesion and proliferation on titanium with hydrothermally treated nanocrystalline hydroxyapatite/magnetically treatedarbon nanotubes *J. Nanosci. Nanotechnol.* **12** 7692–702

[94] Faccio G, Kämpf M M, Piatti C, Thöny-Meyer L and Richter M 2014 Tyrosinase-catalyzed site-specific immobilization of engineered C-phycocyanin to surface *Sci. Rep.* **4** 5370–5

[95] Yang S H, Hong D, Lee J, Ko E H and Choi I S 2013 Artificial spores: cytocompatible encapsulation of individual living cells within thin, tough artificial shells *Small* **9** 178–86

[96] Cabral J M S, Novais J M and Kennedy J F 1986 Immobilization studies of whole microbial cells on transition metal activated inorganic supports *Appl. Microbiol. Biotechnol.* **23** 157–62

[97] Oncescu V and Erickson D 2013 High volumetric power density, non-enzymatic, glucose fuel cells *Sci. Rep.* **3** 1226

[98] Yu H, Tang H and Xu P 2014 Green strategy from waste to value-added-chemical production: efficient biosynthesis of 6-hydroxy-3-succinoyl-pyridine by an engineered biocatalyst *Sci. Rep.* **4** 5397

[99] Olejnik M, Twardowska M, Zaleszczyk W and Mackowski S 2012 Bio conjugation of silver nanowires with photosynthetic, light-harvesting complexes *Acta Phys. Pol.* A **122** 357–60

[100] Goldys E and Xie F 2008 Metallic nanomaterials for sensitivity enhancement of fluorescence detection *Sensors* **8** 886–96

[101] Shanmukh S, Jones L, Driskell J, Zhao Y, Dluhy R and Tripp R A 2006 Rapid and sensitive detection of respiratory virus molecular signatures using a silver nanorod array SERS substrate *Nano Lett.* **6** 2630–6

[102] Dohyun K and Amy E H 2013 Protein immobilization techniques for microfluidic assays *Biomicrofluidics* **7** 041501

[103] Delgado J M P 2006 A critical review of dispersion in packed beds *Heat Mass Transfer* **42** 279–10

[104] Quiros M, Garcia A B and Montes-Moran M A 2011 Influence of the support surface properties on the protein loading and activity of lipase/mesoporous carbon biocatalysts *Carbon* **49** 406–15

[105] Grzelakowski M, Onaca O, Rigler P, Kumar M and Meier W 2009 Immobilized protein–polymer nanoreactors *Small* **5** 2545–8

[106] Temino D M, Hartmeier W and Ansorge-Schumacher M B 2005 Entrapment of the alcohol dehydrogenase from Lactobacillus kefir in polyvinyl alcohol for the synthesis of chiral hydrophilic alcohols in organic solvents *Enzyme Microb. Technol.* **36** 3–9

[107] Qiu H, Li Y, Ji G, Zhou G, Huang X, Qu Y and Gao P 2009 Immobilization of lignin peroxidase on nanoporous gold: enzymatic properties and *in situ* release of H_2O_2 by coim-mobilized glucose oxidase *Bioresour. Technol.* **100** 3837–42

[108] Kim J, Grate J W and Wang P 2006 Nanostructures for enzyme stabilization *Chem. Eng. Sci.* **61** 1017–26

[109] Li J, Cheng X, Shashurin A and Keidar M 2012 Review of electrochemical capacitors based on carbon nanotubes and graphene *Graphene* **1** 1–12

[110] Kumar S, Levchenko I, Cheng Q J, Shieh J and Ostrikov K 2012 Plasma enables edge-to-center-oriented graphene nanoarrays on Si nanograss *Appl. Phys. Lett.* **100** 053115

[111] Chauhan N and Narang J 2013 Immobilization of lysine oxidase on a gold–platinum nanoparticles modified Au electrode for detection of lysine *Enzyme Microb. Technol.* **52** 265–71

[112] Song Z, Yuan R, Chai Y, Jiang W, Su H, Che X and Ran X 2011 Simultaneous immobilization of glucose oxidase on the surface and cavity of hollow gold nanospheres as labels for highly sensitive electrochemical immunoassay of tumor marker *Biosens. Bioelectron.* **26** 2776–80

[113] Petkova G A, Záruba K, Zvátora P and Král V 2012 Gold and silver nanoparticles for biomolecule immobilization and enzymatic catalysis *Nanoscale Res. Lett.* **7** 1–10

[114] Ding K, Liu L, Cao Y, Yan X, Wei H and Guo Z 2014 Formic acid oxidation reaction on a PdxNiy bimetallic nanoparticle catalyst prepared by a thermal decomposition process using ionic liquids as the solvent *Int. J. Hydrog. Energy* **39** 7326–37

[115] Sun Y 2010 Silver nanowires—unique templates for functional nanostructures *Nanoscale* **2** 1626–42

[116] Davoudi Z M, Kandjani A E, Bhatt A I, Kyratzis I L, O'Mullane A P and Bansal V 2014 Hybrid antibacterial fabrics with extremely high aspect ratio Ag/AgTCNQ nanowires *Adv. Funct. Mat.* **24** 1047–53

[117] Gunawan C, Teoh W. Y, Marquis C P, Lifia J and Amal R 2009 Reversible antimicrobial photoswitching in nanosilver *Small* **5** 341–4

[118] Levchenko I, Ostrikov K and Murphy A B 2008 Plasma-deposited Ge nanoisland films on Si: is Stranski–Krastanow fragmentation unavoidable? *J. Phys. D: Appl. Phys.* **41** 092001

[119] Yu L, Zhang Y, Zhang B and Liu J 2014 Enhanced antibacterial activity of silver nanoparticles/halloysite nanotubes/graphene nanocomposites with sandwich-like structure *Sci. Rep.* **4** 4551

[120] Baksi A, Xavier P L, Chaudhari K, Goswami N, Pal S K and Pradeep T 2013 Protein-encapsulated gold cluster aggregates: the case of lysozyme *Nanoscale* **5** 2009–16

[121] Fang J, Levchenko I and Ostrikov K 2015 Atmospheric plasma jet-enhanced anodization and nanoparticle synthesis *IEEE Trans. Plasma Sci.* **43** 765–9

[122] Xu S, Long J, Sim L, Diong C H and Ostrikov K 2005 RF plasma sputtering deposition of hydroxyapatite bioceramics: synthesis, performance, and biocompatibility *Plasma Proc. Polym.* **2** 373–90

[123] Yan T, Zhong X, Rider A E, Lu Y, Furman S A and Ostrikov K 2014 Microplasma-chemical synthesis and tunable real-time plasmonic responses of alloyed Au_xAg_{1-x} nanoparticles *Chem. Commun.* **50** 3144

[124] Askari S, Svrcek V, Maguire P and Mariotti D 2015 The interplay of quantum confinement and hydrogenation in amorphous silicon quantum dots *Adv. Mater.* **27** 8011–6

[125] Costerton J W, Lewandowski Z, Caldwell D E, Korber D R and Lappinscott H M 1995 Microbial biofilms *Annu. Rev. Microbiol.* **49** 711–45

[126] Lee K C and Rittmann B E 2002 Applying a novel autohydro-genotrophic hollow-fiber membrane biofilm reactor for denitrification of drinking water *Water Res.* **36** 2040–52

[127] San N O, Celebioglu A, Tumtas Y, Uyar T and Tekinay T 2014 Reusable bacteria immobilized electrospun nanofibrous webs for decolorization of methylene blue dye in wastewater treatment *RSC Adv.* **4** 32249–55

[128] Gupta R, Gigras P, Mohapatra H, Goswami V K and Chauhan B 2003 Microbial alpha-amylases: a biotechnological perspective *Process Biochem.* **38** 1599–16

[129] Logan B E 2009 Exoelectrogenic bacteria that power microbial fuel cells *Nat. Rev. Microbiol.* **7** 375–81

[130] Burgess J G, Boyd K G, Armstrong E, Jiang Z, Yan L M and Berggren M 2003 The development of a marine natural product-based antifouling paint *Biofouling* **19** 197–205

[131] Chambers L D, Stokes K R, Walsh F C and Wood R J K 2006 Modern approaches to marine antifouling coatings *Surf. Coat. Technol.* **201** 3642–52

[132] Costerton J W, Stewart P S and Greenberg E P 1999 Bacterial biofilms: a common cause of persistent infections *Science* **284** 1318–22

[133] Fang J, Levchenko I, Mai-Prochnow A, Keidar M, Cvelbar U, Filipic G, Han Z J and Ostrikov K 2015 Protein retention on plasma-treated hierarchical nanoscale gold-silver platform *Sci. Rep.* **5** 13379

[134] Vecitis C D, Zodrow K R, Kang S and Elimelech M 2010 Electronic-structure-dependent bacterial cytotoxicity of single-walled carbon nanotubes *ACS Nano* **4** 5471–9

[135] Mai-Prochnow A, Bradbury M, Ostrikov K and Murphy A B 2015 *Pseudomonas aeruginosa* biofilm response and resis-tance to cold atmospheric pressure plasma is linked to the redox-active molecule phenazine *PLoS One* **10** e0130373

[136] Li Y, Zhang Y and Yan B 2014 Nanotoxicity overview: nano-threat to susceptible populations (Review) *Int. J. Mol. Sci.* **15** 3671–97

[137] Fratoddi I, Venditti I, Cametti C and Russo M V 2015 How toxic are gold nanoparticles? The state-of-the-art *Nano Res.* **8** 1771–99

[138] Yah C S 2013 The toxicity of gold nanoparticles in relation to their physiochemical properties *Biomed. Res.* **24** 400–13

[139] Kiliç G, Costa C, Fernández-Bertólez N, Pásaro E, Teixeir J P, Laffon B and Valdiglesias V 2016 *In vitro* toxicity evaluation of silica-coated iron oxide nanoparticles in human SHSY5Y neuronal cells *Toxicol. Res.* **5** 235–47

[140] Nguyen K C, Seligy V L, Massarsky A, Moon T W, Rippstein P, Tan J and Tayabali A F 2013 Comparison of toxicity of uncoated and coated silver nanoparticles *J. Phys.: Conf. Ser.* **429** 012025

[141] Suresh A K, Pelletier D A, Wang W, Morrell-Falvey J L, Gu B and Doktycz M J 2012 Cytotoxicity induced by engineered silver nanocrystallites is dependent on surface coatings and cell types *Langmuir* **28** 2727–35

[142] Mendes R G *et al* 2014 Synthesis and toxicity characterization of carbon coated iron oxide nanoparticles with highly defined size distributions *Biochim. Biophys. Acta* **1840** 160–9

[143] Yoon O J, Kim I, Sohn I Y, Kieu T T and Lee N E 2014 Toxicity of graphene nanoflakes evaluated by cell-based electrochemical impedance biosensing *J. Biomed. Mater. Res.* A **102** 2288–94

[144] Bradley D 2012 Is graphene safe? *Mater. Today* **15** 230

[145] Yildirimer L, Thanh N T K, Loizidou M and Seifalian A M 2011 Toxicology and clinical potential of nanoparticles *Nanotoday* **6** 585–607

[146] Nel A, Xia T, Madler L and Li N 2006 Toxic potential of materials at the nanolevel *Science* **311** 622–7

[147] Czajkowska B and Blazewicz M 1997 Phagocytosis of chemically modified carbon materials *Biomaterials* **18** 69–74

[148] Simeonova P P 2009 Update on carbon nanotube toxicity *Nanomedicine* **4** 373–5

[149] Han Z J, Levchenko I, Kumar S, Yajadda M M A, Yick S, Seo D H, Martin P J, Peel S, Kuncic Z and Ostrikov K 2011 Plasma nanofabrication and nanomaterials safety *J. Phys. D: Appl. Phys.* **44** 174019

[150] Yan D, Talbot A, Nourmohammadi N, Sherman J H, Cheng X and Keidar M 2015 Toward understanding the selective anticancer capacity of cold atmospheric plasma—a model based on aquaporins *Biointerphases* **10** 040801

[151] Siu A, Volotskova O, Cheng X, Khalsa S S, Bian K, Murad F, Keidar M and Sherman J H 2015 Differential effects of cold atmospheric plasma in the treatment of malignant glioma *PLoS One* **10** e0126313

[152] Keidar M 2015 Plasma for cancer treatment *Plasma Sources Sci. Technol.* **24** 033001

[153] Cheng X, Rajjoub K, Sherman J, Canady J, Recek N, Yan D, Bian K, Murad F and Keidar M 2015 Cold plasma accelerates the uptake of gold nanoparticles into glioblastoma cells *Plasma Process. Polym.* **12** 1364–9

[154] Shashurin A, Scott D, Zhuang T, Canady J, Beilis I I and Keidar M 2015 Electric discharge during electrosurgery *Sci. Rep.* **4** 9946

[155] Yan D, Talbot A, Nourmohammadi N, Cheng X, Canady J, Sherman J and Keidar M 2015 Principles of using cold atmospheric plasma stimulated media for cancer treatment *Sci. Rep.* **5** 18339

[156] Recek N, Cheng X, Keidar M, Cvelbar U, Vesel A, Mozetic M and Sherman J 2015 Effect of cold plasma on glial cell morphology studied by atomic force microscopy *PLoS One* **10** e0119111

[157] Shashurin A, Keidar M, Bronnikov S, Jurjus R A and Stepp M A 2008 Living tissue under treatment of cold plasma atmospheric jet *Appl. Phys. Lett.* **93** 19529842